

**Contract No:**

This document was prepared in conjunction with work accomplished under Contract No. DE-AC09-08SR22470 with the U.S. Department of Energy.

**Disclaimer:**

This work was prepared under an agreement with and funded by the U.S. Government. Neither the U. S. Government or its employees, nor any of its contractors, subcontractors or their employees, makes any express or implied: 1. warranty or assumes any legal liability for the accuracy, completeness, or for the use or results of such use of any information, product, or process disclosed; or 2. representation that such use or results of such use would not infringe privately owned rights; or 3. endorsement or recommendation of any specifically identified commercial product, process, or service. Any views and opinions of authors expressed in this work do not necessarily state or reflect those of the United States Government, or its contractors, or subcontractors.

## **Impact of Nuclear Material Dissolution on Vessel Corrosion**

**J. I. Mickalonis, K. A. Dunn, W. R. Clifton**  
**Savannah River National Laboratory**  
**Savannah River Nuclear Solutions**  
**Aiken, SC 29808**

### **Abstract**

Different nuclear materials require different processing conditions. In order to maximize the dissolver vessel lifetime, corrosion testing was conducted for a range of chemistries and temperature used in fuel dissolution. Compositional ranges of elements regularly in the dissolver were evaluated for corrosion of 304L, the material of construction. Corrosion rates of AISI Type 304 stainless steel coupons, both welded and non-welded coupons, were calculated from measured weight losses and post-test concentrations of soluble Fe, Cr and Ni.

Keywords: stainless steel, nitric acid, IGA

### INTRODUCTION

A flowsheet was developed for the dissolution of the Sand, Slag, and Crucible (SS&C) materials in a dissolvers [1]. This flowsheet differs slightly from previous ones developed for sand, slag and crucible [2]. A corrosion testing program was initiated to study the effect of various process parameters, including temperature and the composition of the dissolution solution [3]. This report discusses only the corrosion rates at 30 and 90 °C.

The corrosion testing program consisted of batch-type coupon immersion tests performed with prototypical material in solutions, which covered an array of compositions. These compositions bracketed those in the SS&C flowsheet. The primary test variables and their values were as follows: nitric acid concentration, 8-10 M; fluoride concentration, 0.2-0.7 M; temperatures of 30 and 90 °C; boron concentration, 1.6-2.0 g/L; iron concentration, 0-0.18 M. Additional variables were the material composition, AISI Type 304L and 304 stainless steels, and fabrication techniques, non-welded and welded. The material variables were used to establish a degree of conservatism in the corrosion rate estimates.

### EXPERIMENTAL SETUP

An important aspect of the experimental program was determining the “effective” fluoride concentration. Experimental testing related to the development of the SRS SS&C flowsheet showed that the dissolution and corrosion processes were more closely correlated to an “effective” free fluoride concentration rather than the total molar fluoride concentration [2]. The fluoride ions in solution are complexed primarily by the boron, which is added as a nuclear poison. This complexing reduces the fluoride concentration

active in dissolution and corrosion, or, in other words, reduces the “effective” free fluoride concentration. Iron and hydronium ions may have a similar, albeit smaller, impact. The free fluoride concentrations, as discussed below, were measured with an ion selective electrode.

#### Solution Preparation

The compositional ranges for the test solutions bracketed the developed flowsheet and are shown in Table 1. Solution preparation was performed using task specific instructions. For each acid concentration, similar fluoride concentrations were used. The fluoride source was calcium fluoride (CaF<sub>2</sub>). The boron, which was added as boric acid (H<sub>3</sub>BO<sub>3</sub>), was a constant for most tests at a concentration of 2.0 g/L. Solutions with a boron concentration of 1.6 g/L were limited to molar fluoride concentrations of 0.3 and 0.7. Most tests contained the maximum iron concentration of 0.18 M. A single test was performed with no iron at each molar acid concentration. The iron was added as ferric nitrate (Fe(NO<sub>3</sub>)<sub>3</sub>·9H<sub>2</sub>O). The solutions were made from reagent grade chemicals. The testing was performed in three series of tests, two at 90 °C and one at 30 °C. All solutions were not tested during each series. Appendix 1 lists the specific solutions for each series.

The solutions were made from master solutions for each of the molar acid concentrations, 8, 9, and 10 M. The master solutions were made using concentrated nitric acid. Chemicals were added sequentially in the following order: H<sub>3</sub>BO<sub>3</sub>, Fe(NO<sub>3</sub>)<sub>3</sub>·9H<sub>2</sub>O, and CaF<sub>2</sub>. The master solutions were heated to approximately 40 °C to facilitate dissolution of the chemicals. The solutions were made in glassware and transferred immediately to polyethylene or Teflon® bottles, so as to minimize solution contamination. Analyses of the fluoride concentration and overall solution chemistry were performed prior to and after testing. These analyses are described in the section on solution analysis.

**Table 1. Concentration Ranges Of Simulated Dissolver Solutions For RFSS&C**

<b>Constituent</b>	<b>High Concentration (M)</b>	<b>Low Concentration (M)</b>
Nitric acid	10	8
Fluoride	0.7	0.2
Iron	0.18	0
Boron	2.0 g/L	1.6 g/L

#### Coupon Preparation

The dissolver is made from AISI Type 304L (304L) stainless steel. 304L is a low carbon alternative to Type 304 (304) stainless steel. The dissolver was fabricated with several types of welds. The microstructure and composition of the weld region differs from those of the base material. These differences can impact the corrosion resistance. The test coupons were chosen to simulate both the weld region and the base material.

Several coupon types and materials were used including non-welded 304L, and both welded and non-welded 304. The 304 coupons were used because of availability and time

restraints for testing. The lower carbon content for 304L minimizes carbide precipitation in the heat-affected zones of the weld region. Carbide precipitates make the material more susceptible for intergranular attack [8]. Therefore, the 304 coupons provided an added measure of conservatism to the testing.

The nominal dimensions of the coupons were as follows: 304L non-welded, 0.9" × 2.0" × 0.0625"; 304 welded, 1.0" × 2.0" × 0.0625" with a 0.25" central hole; and 304 non-welded, 0.75" × 3.0" × 0.125". The surface of each coupon was prepared using standard metallographic techniques to obtain a 600 grit surface finish. Each coupon was weighed on a calibrated digital balance to the ten thousandth decimal place (0.0000 g). After weighing, a Teflon® string was attached to each coupon through the small hole near one end. All coupons were stored in a dessicator until placed into test.

### Test Procedure

Teflon® bottles were used as the test vessels for solution containment. Teflon® was chosen because of its chemical and thermal resistance at 30 and 90 °C. For most tests, a welded and a non-welded coupon were hung in each bottle. In the second series at 90 °C, some tests were performed with the non-welded 304 and 304L coupons. The coupons were attached to the bottle lid to facilitate removal for weighing. Each coupon was suspended to ensure complete immersion in the solution. Teflon® tape was used on the bottleneck to minimize evaporation. The bottles were placed in an oven on a stainless steel or glass tray.

Weight measurements were taken after one day and at the end of the exposure period, which was one week. The weighing process entailed removing bottles individually from the oven. The coupons were detached, rinsed with distilled water, and dried by forced air prior to weighing. For the one-day measurement, the coupons were re-attached to the cap, immersed in the same solution, and placed back into the oven for the remainder of the test. At the end of the test, each coupon was then stored in a dessicator for further metallurgical evaluation.

The volumes of the test solutions were also measured because of evaporation. Typically, the final solution volume was between 350-450 ml. The ratio of initial to final "effective" free fluoride concentrations was found to be smaller with greater evaporation, i.e. smaller final volumes. Although the free fluoride concentration dropped because of consumption in the dissolution process, some fluorides may also volatilize during evaporation.

### Solution Analyses

The solutions were analyzed for the following constituents: Al, Fe, Cr, Ni, and B by Ion Chromatograph Plasma Enhanced Spectroscopy (ICPES); nitrates, chlorides, and total fluorides by Ion Chromatograph for Anions; fluoride by Ion Selective Electrode (ISE), and total acid by titration. For the ISE measurements, a buffer was added to the test

samples to neutralize the pH and break the complexes formed with fluorides by aluminum and iron. The Fe, Cr, and Ni results were used to calculate a corrosion rate as discussed in the Analysis section

#### Free Fluoride Measurements

The “effective” free fluoride concentration was measured in the test solutions using the ISE technique. The terminology of “effective” free fluoride is used because solution fluoride is complexed by the iron, boron, and hydronium ions. These fluoride atoms are not active in the dissolution and corrosion processes. Therefore, the “effective” free fluoride concentration consists of those fluoride ions available for these processes. These measurements were made without buffering as done by the analytical laboratory so as to have an estimate of this available fluoride concentration

The ISE measurement is a solution potential (mV) which varies depending on solution composition, i.e. fluoride concentration. A calibrating curve was developed to correlate the solution potential to a specific fluoride concentration. The correlation is a linear relationship between the measured solution potential and the logarithm of the fluoride concentration.

Standard calibrating solutions were prepared containing a range of calcium fluoride concentrations, 9.5, 47.5, 95, 475, 950, and 4750 ppm, in each of the molar acid concentrations (8, 9, and 10 M). These calibrating solutions matched the test solution matrix, i.e. molar acid concentration, which affects the “effective” free fluoride concentration. Note that these fluoride values are not the actual free fluoride since the fluoride ions are not dissociated from the hydronium ions in these concentrated acid solutions.

For each acid concentration, the standard solutions were made from a master solution with the largest fluoride concentration and serially diluted to obtain the lower concentration standards. During the tedious preparation of these standard solutions, care was exercised to minimize cross contamination of containers or stirring medium. The calibrating solutions were stored in labeled polyethylene bottles.

ISE measurements were made with an Accumet Model 50 meter with an Orion Ion Plus combination fluoride electrode. The procedure for making an ISE measurement of both the calibrating and test solutions involved thoroughly rinsing the electrode, allowing the meter response to stabilize, and recording the voltage readout. For the standard solutions, the voltage measurements were plotted against the solution fluoride concentration to verify the linear relationship. Figure 1 shows the calibrating curve generated with the standards at 8, 9, and 10 M nitric acid concentrations. The calibrating curve was always checked prior to measurements of the test solutions. All ISE measurements were made at ambient temperature.

### Coupon Analysis

The coupons were evaluated visually for characterizing the corrosion process(es). Photographs of the coupons were taken to document the post-test condition. Both welded and non-welded coupons were evaluated on a microscopic scale using standard metallographic techniques. The coupons were sectioned transversely to the length, mounted in an epoxy resin, ground, and polished. Prior to observation, the coupons were electrolytically etched with a 10 wt% oxalic acid solution. The degradation and microstructure were evaluated using an optical metallograph. Micrographs were taken to document the findings.

### ANALYSIS

The corrosion rate was calculated from both a coupon weight loss and the concentration of soluble Fe, Cr, and Ni ions in a test solution. The corrosion rate based on the soluble ion concentration was used to verify the rate based on the weight loss. When 304 stainless steel corrodes, the soluble species in an acid solution are iron, chromium, and nickel. As explained in the Experimental Section, coupon weights were measured prior to testing, after a one-day exposure, and at the end of the test (a one-week exposure). A short-term and extended corrosion rate were calculated from the one-day and one-week data, respectively. The soluble ion concentrations were measured at the end of the test for calculating only an extended corrosion rate.

The corrosion rate (CR) in mils per year (mpy) was calculated from the following equation [8]:

$$CR = (C \times W) / (\rho \times A \times T) ; \quad (1)$$

where C is a corrosion constant ( $3.45 \times 10^6$ ), W is either the weight loss (g) from the coupons or the total accumulated weight (g) of soluble Fe, Cr, and Ni,  $\rho$  is the density of 304 and 304L stainless steel (7.94 g/cc), A is the surface area of the coupon ( $\text{cm}^2$ ), and T is the time (hr) of exposure, either 24 or 168 hours.

The method for calculating the corrosion rate based on the soluble ions concentrations consisted of adjusting the final concentrations by subtracting the initial concentrations of these species. This approach was required because of the addition of iron nitrate to the test solutions. The initial Cr and Ni concentrations were insignificant. The surface area used in this calculation was the total surface area of the two exposed coupons. The calculated rate, therefore, was an average for the two coupons.

### RESULTS AND DISCUSSION

The calculated corrosion rates in prototypical dissolver solutions were strongly correlated to most of the test variables, which were related to important process parameters. A direct

relationship was found with the temperature and the fluoride and nitric acid concentrations. An inverse relationship was found between the corrosion rate and the boron concentration. The coupon condition also affected the corrosion rate where, in general, higher rates were measured for welded coupons. The material composition and solution iron concentration had minimal or insignificant effects on the corrosion rate. All these relationships were found for both the short-term and extended corrosion rates. These relationships are discussed at length below.

Calculated Corrosion Rates

Corrosion rates were calculated for all test conditions based on weight loss measurements using Equation (1). Table 2 shows the average range of corrosion rates of non-welded 304L coupons for the most likely process variables of 2.0 g/L boron and 0.18M iron at 90°C. Ranges are shown for each molar acid concentration. The average rate at 9M nitric acid with 0.7M fluoride was lower than the 8M solution because of an unusually low rate in the first test series. Similar data is shown in Table 3 for the welded 304 coupons.

Table 2. Average Corrosion Rates Of Non-welded 304L

Nitric Acid (M)	Corrosion Rate (mpy)	
	0.2 M Fluoride	0.7 M Fluoride
8	31.4	113.8
9	36.1	108.4
10	44.2	132.6

Table 3. Average Corrosion Rates Of Welded 304

Nitric Acid (M)	Corrosion Rate (mpy)	
	0.2 M Fluoride	0.7 M Fluoride
8	34.6	132.7
9	41.7	145.0
10	51.1	174.3

The short-term rate was expected to be greater than the extended rate since rates tend to be higher during the initial periods prior to the formation of corrosion products and the stabilization of the system. This result was found to be true for the non-welded coupons. Short-term corrosion rates were greater by an average of 2.5 mpy than the extended rates, although there was a large degree of variability.

For the welded coupons the extended rates were greater than the short-term rates by an average of 13 mpy. The higher rates resulted from the intergranular attack (IGA) that

occurred at longer times. The IGA lead to grain pullout. Figure 2 is a plot of the corrosion rate as a function of molar fluoride concentration for the welded coupons in the first test series. Figure 3 is the same corrosion rate data but plotted versus the “effective” free fluoride concentration. The short-term rate is plotted versus the initial free fluoride measurement, while the extended rate is plotted versus the final free fluoride measurement. An additional factor may be the type of corrosion. As discussed below, the welded coupons had more significant corrosion, which tended to be intergranular in nature. As the corrosion proceeded, a greater surface was exposed, thereby leading to more corrosion and the greater corrosion rate.

Reproducibility of results was not entirely consistent and was attributed to coupon variability. In the series 1 and series 2 corrosion tests, the 304L non-welded coupons were resurfaced by hand before each test, which produced a non-uniform surface. As a result, test coupon surfaces were not reproducible and lead to data variability. This variability is shown in Figure 4 where the corrosion rates from the second series were higher than the first series, even though the test conditions were identical. In contrast, a new welded 304 coupon was used for each series and had the original machine finish. Corrosion rates from these tests were consistent and followed the expected trend for these coupons. New coupons were used for the remainder of the tests.

#### Nitric Acid and Fluoride Concentrations

The corrosion rates of 304L and 304 stainless steels are strongly impacted by both the fluoride and nitric acid concentration, increasing rates resulted from increasing concentrations. Figure 2 shows the corrosion rate as a function of molar fluoride concentration for welded 304 coupons from the first test series at a temperature of 90 °C. The change in molar fluoride concentration has a greater effect on the corrosion rate than the molar acid concentration.

The functional relationship between corrosion rate and fluoride concentration changes when the “effective” free fluoride concentration is used. Figure 3 shows this relationship using the same data from Figure 2. Corrosion rate still increases with both fluoride and acid concentration. Larger fluoride concentrations (0.6 and 0.7 M) have significantly larger free fluoride concentrations, indicating a possible limit to the effect of complexing by boron as discussed below.

#### Effect of Material Composition and Fabrication

Both 304L and 304 stainless steels were tested in the non-welded condition. Surprisingly the 304L had greater corrosion rates than the 304. For the 90 °C tests, this difference was 10 mpy at 0.3 M fluoride and 40 mpy at 0.7 M fluoride, independent of acid concentration. The coupons had similar microstructural characteristics as discussed in the section on coupon characterization. Figure 5 shows this relationship as a function of “effective” free fluoride concentration.

An important consideration for the dissolver is the degradation of the weld regions, which tend to be the most susceptible areas to corrosion. For the corrosion tests outlined in this report, the expected trend was observed, in most cases, and the weld regions were found to have a greater corrosion rate than non-welded regions. This increased corrosion rate, as discussed below in Section 5.6, was caused by the microstructural differences that were an outcome of the welding process. A variance from the expected trend, however was observed in some of the tests, specifically the series 1 and series 2 tests using the 304L coupons. For the first test series, the non-welded 304L corrosion rates were on average 3 mpy greater than those of the welded 304 coupons. In the second series, the non-welded 304L corrosion rates were approximately 38 mpy greater than those of the welded 304 coupons. In contrast to that, the 304 welded coupons had a corrosion rate that was, on average, 64 mpy greater than those of the 304 non-welded coupon corrosion rates, both of which were tested at the same conditions as the 304L coupons. This observed difference may be related to the non-reproducible surfaces on the 304L coupons (see Section 5.1).

#### Effect of Boron and Iron on Corrosion Rate

The boron concentration effects the free fluoride concentration of the dissolver solution. Lower free fluoride occurs with larger boron concentrations due to the complexing reaction between the two ions. Therefore, higher corrosion rates resulted when the boron concentration was changed from 2.0 to 1.6 g/L in these tests. When corrosion rate is plotted versus the “effective” free fluoride concentration, this effect is clearly demonstrated as shown in Figure 6 for 304 non-welded coupons.

Iron was expected to affect the corrosion rate either negatively or positively, depending on the strength of two countering processes. Iron also complexes fluoride, so an effect similar to the addition of adding boron could have occurred, although boron is a stronger complexant. The ferric ions in solution may have also accelerated corrosion if it acted as a reductant accelerating the cathodic reaction of the corrosion process. The corrosion rate, however, was unaffected by the complete removal of iron as shown in Figure 6.

#### Solution Analysis

Solution analyses were performed to measure the soluble Fe, Cr and Ni concentrations and verify solution chemistries. The target fluoride concentrations were found to be in good agreement with the analytical results. Corrosion rate calculations were based on the total weight of Fe, Ni, and Cr measured in the solutions. Pre-test quantities were subtracted from the post-test quantities to obtain the adjusted concentrations. These adjusted quantities were summed and used as the weight loss shown in Equation 1. For these corrosion rate calculations the surface area was the combined surface area for the welded and non-welded coupons. The average corrosion rate calculated from the coupon weight loss agrees relatively well with the solution analysis corrosion rate and hence is validated.

### Coupon Characterization

The visual observation of the 304L and 304 coupons showed general corrosion on the non-welded coupons. The corrosion of the welded coupons, however, was more significant. Figure 7 shows a representative photograph of a group of welded coupons that were exposed to a 10 M nitric acid solution with 0.2-0.7 M fluoride, 2.0 g/L boron, and 0.18 M iron at 90 °C. The weld is clearly evident on the welded coupons indicating either a buildup of corrosive product or greater attack of the weld by the dissolver solution. The visual appearance of the base metal from the welded coupons and the entire surface of the non-welded coupons indicated general corrosion attack.

The microstructural characteristics of the coupon material and the morphological details of the corrosion process were evaluated for both a welded and a non-welded coupon. Figure 8 shows the photomicrographs of these coupons, which are typical for all test coupons. The coupons show the effect of corrosion on the surface of each sample. Figure 9 shows a transverse cross section of a 304 welded coupon. The exposed edge at the weld appears to exhibit general corrosion and does not indicate the presence of severe corrosion at the welded region itself. The edge of the coupon in the parent metal region, however, shows the presence of primarily InterGranular Attack (IGA) from the testing solution. In addition, precipitates are seen dispersed throughout the parent metal matrix.

IGA is caused by impurities at the grain boundaries causing the grain boundary to be more reactive than the matrix. This type of attack is generally associated with sensitization in 304 stainless steel, where chromium carbides form at the grain boundaries. Formation of these carbides depletes the surrounding area of chromium. This chromium-depleted zone provides a region adjacent to the weld that does not contain sufficient corrosion resistance to resist attack in many corrosive environments. Sensitization occurs when certain stainless steels are heated in a temperature range of 950°C to 1450°C. Because of the welding process, these coupons likely saw temperatures in this region. However, because sensitization does not occur in 304L stainless steel, the material of construction for the dissolver vessel, intergranular corrosion will not be a factor in the dissolver vessel. Hence, the IGA seen in the 304 welded coupons should not occur and cause a premature failure in the dissolver vessel. The current testing has welded 304L coupons exposed to the dissolver solutions to verify this hypothesis.

Figure 10 shows a transverse cross section of the 304 non-welded coupon. The exposed edge exhibited the metallographic features of general corrosion on the surface of the coupon. Sensitization of the 304 non-welded coupon was not evident.

### CONCLUSIONS

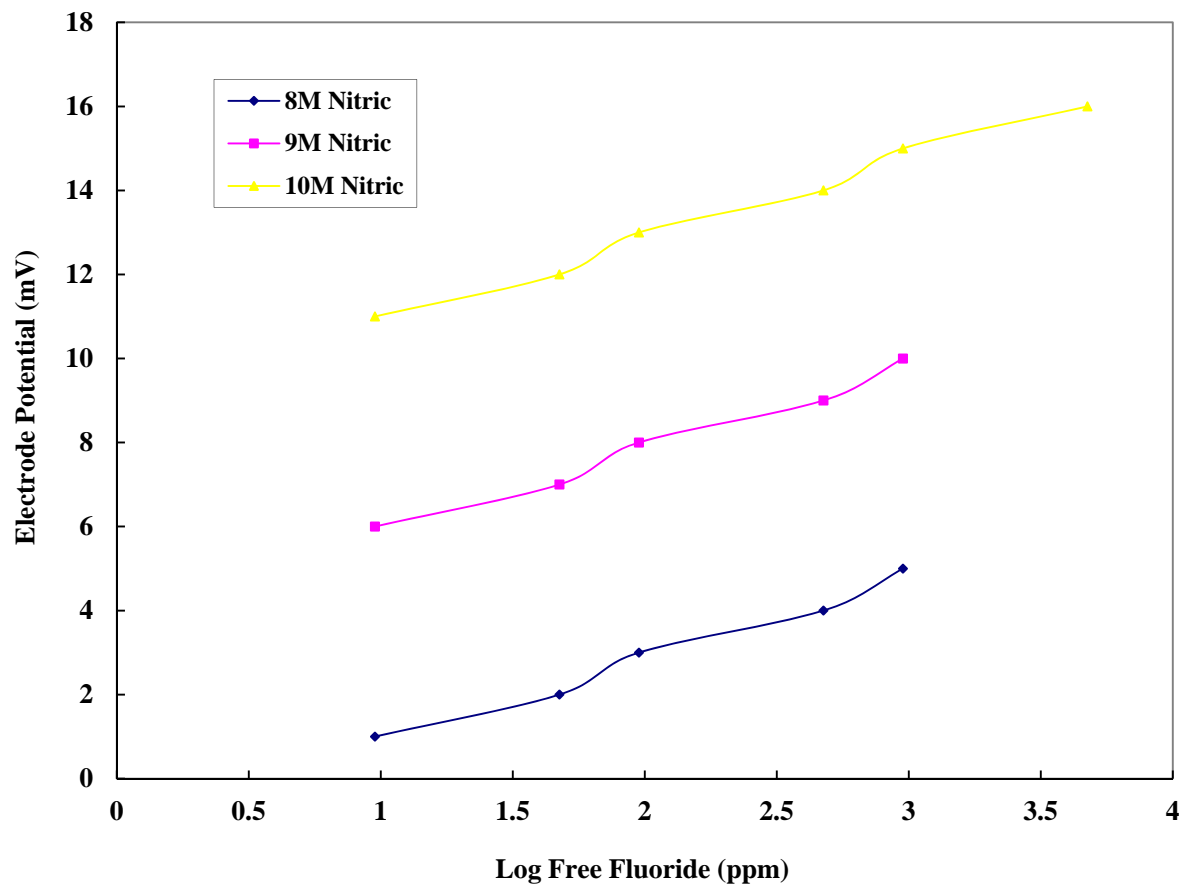
The experimental task for SS&C material consisted of coupon immersion tests in simulated dissolver solutions. The solution chemistries ranges were 8-10 M nitric acid, 0.2-0.7 M calcium fluoride, 2.0 g/L boron, 0-0.18 M iron. Testing was conducted at both 30 and 90 °C. AISI Type 304L and 304 stainless steel coupons were used as representative materials for the dissolver. The coupons were in the non-welded and welded condition.

The measured corrosion rates ranged approximately from 0.2-2.2 mils per year (mpy) for 30 °C and 24-215 mpy for 90 °C. Based on these corrosion rates the corrosion damage to the dissolver would correspond to 0.0005-0.006 mils for a 24 hour campaign at 30°C and 0.07-0.6 mils for a 24 hour campaign at 90°C. The rate increases with the fluoride concentration of the dissolver solution. The actual relationship varies depending on the fluoride value, i.e. a total molar or an “effective” free fluoride concentration. The concentration of boron significantly impacts the free fluoride concentration. Increasing boron concentration lowers the free fluoride concentration at a constant molar fluoride concentration, thereby reducing the corrosion rate. Although iron is known to complex fluoride and reduce the free fluoride concentration, the iron was found to have no effect on either the free fluoride concentration or the corrosion rate when 2.0 g/L of boron was present in the solution. Additionally, welds had higher corrosion rates than non-weld areas, so the most susceptible region for the dissolver will be the fabrication welds.

#### REFERENCES

1. J. H. Gray, “Flowsheets for Processing Sand, Slag, and Crucible Materials in Canyon Dissolvers,” WSRC-TR-99-00360, To be published.
2. “Flowsheet Modifications for Dissolution of Sand, Slag, and Crucible Residues in the F-Canyon Dissolvers,” WSRC-TR-97-00395, December 1997.
3. J. I. Mickalonis, “Corrosion Test Plan: Rocky Flat SS&C Dissolution,” SRT-MTS-99-0217, May, 1999.
4. S. P. Harris, “Statistical Design for F-Canyon Dissolver Work,” SRT-SCS-99-054, July, 1999.
5. Conduct of Research & Development – Savannah River Technology Center (U), WSRC-IM-97-00024, Rev. 1, November 30, 1998.
6. ASTM G31-72, “Standard Practice for Laboratory Immersion Corrosion Testing of Metals,” Annual Book of ASTM Standards, Vol. 3.02, American Society For Testing And Materials, Philadelphia, PA, 1998.
7. NMSS Laboratory notebook, WSRC-NB-97-00510, October 27, 1997 (active notebook).

8. J. D. Sendriks, Corrosion of Stainless Steels, John Wiley & Sons Inc., New York, 1996.
9. R. Baboian (ed), Corrosion Tests and Standards: Application and Interpretation, American Society For Testing and Materials, Philadelphia, PA, 1995.



1.1 FIGURES

**Figure 1. Calibration Curve For Ion Selective Electrode Measurements of Fluoride**

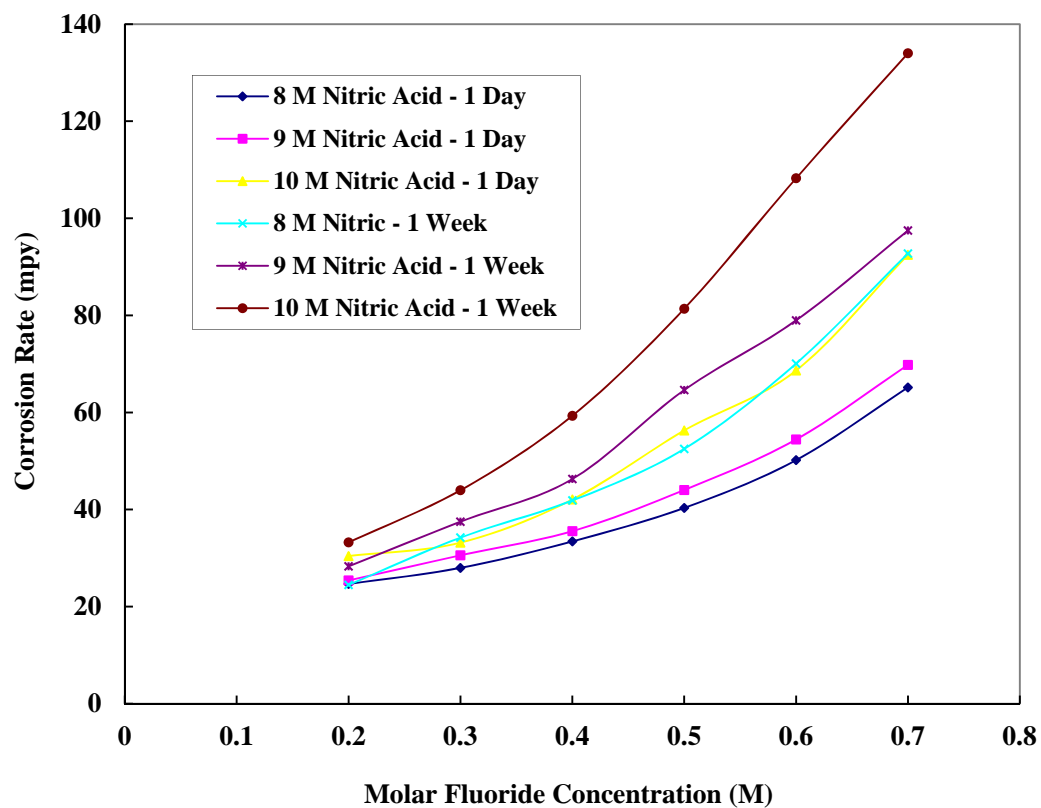


**Figure 2. Corrosion Rate of Welded 304 Coupons At 90 °C – Molar Fluoride Concentration (B=2.0 g/L and Fe=0.18M)**

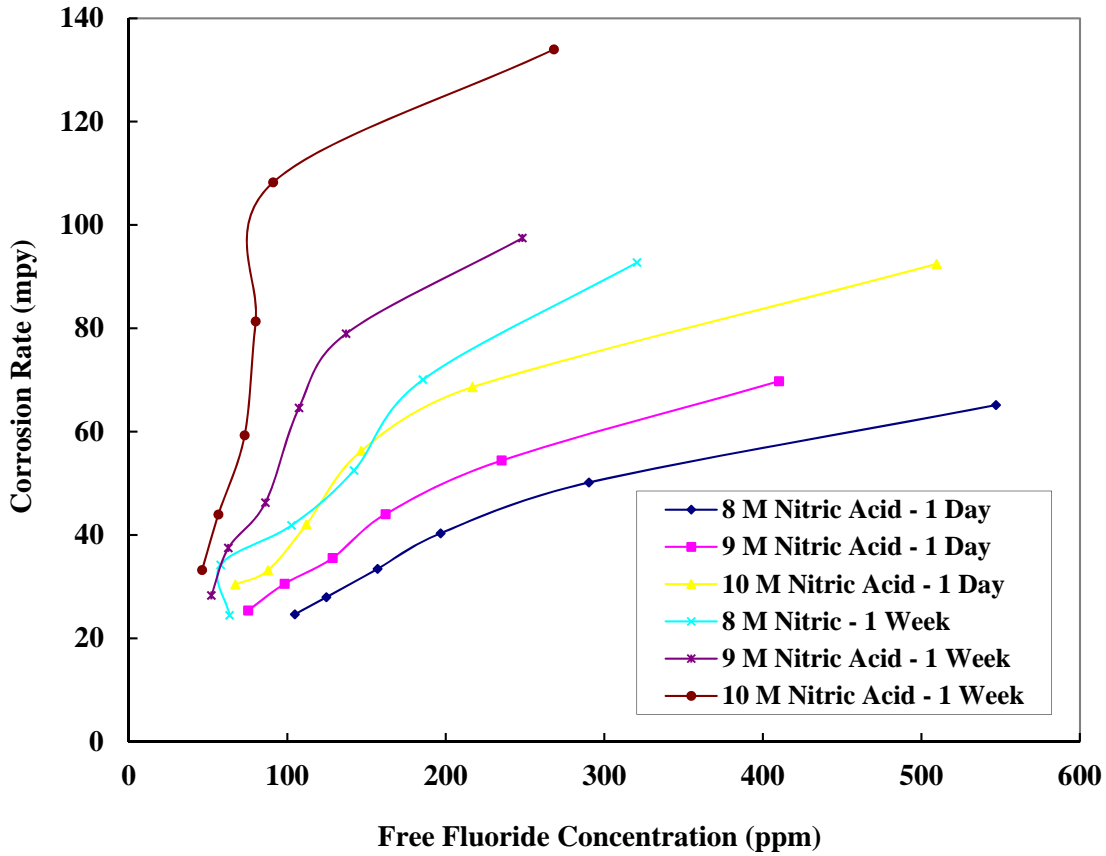


**Figure 3. Corrosion Rate of Welded 304 Coupons At 90 °C – “Effective” Free Fluoride Concentration (B=2.0 g/L and Fe=0.18M)**

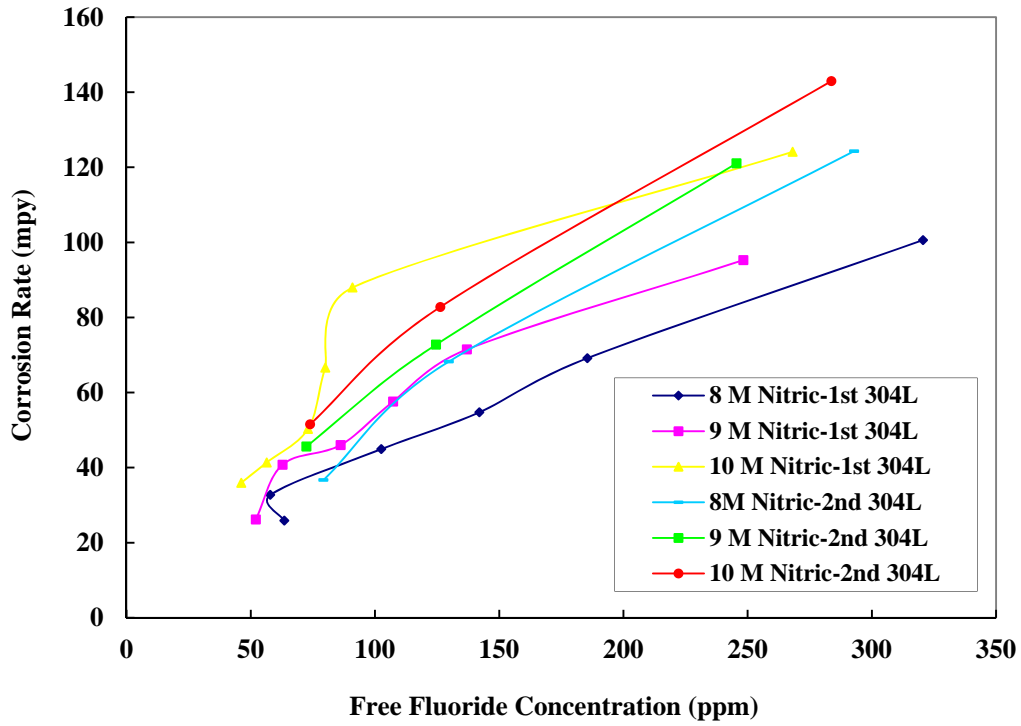


**Figure 4. Corrosion Rate of Non-Welded 304L From the First and Second 90 °C Tests (B=2.0 g/L and Fe=0.18M)**

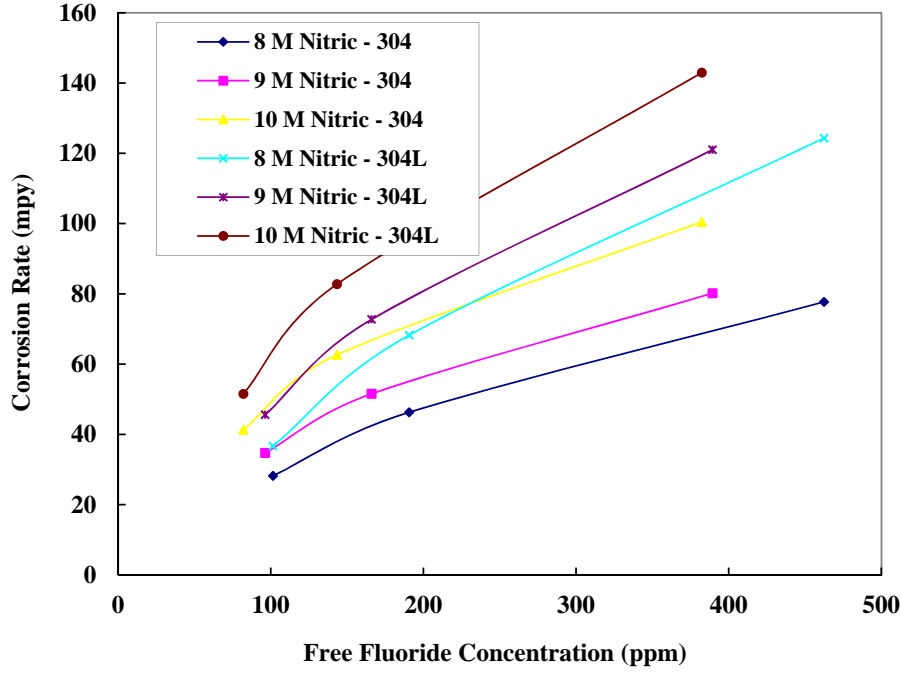


**Figure 5. Corrosion Rates of 304L and 304 Non-welded Coupons From the Second Test At 90 °C (B=2.0 g/L and Fe=0.18M)**

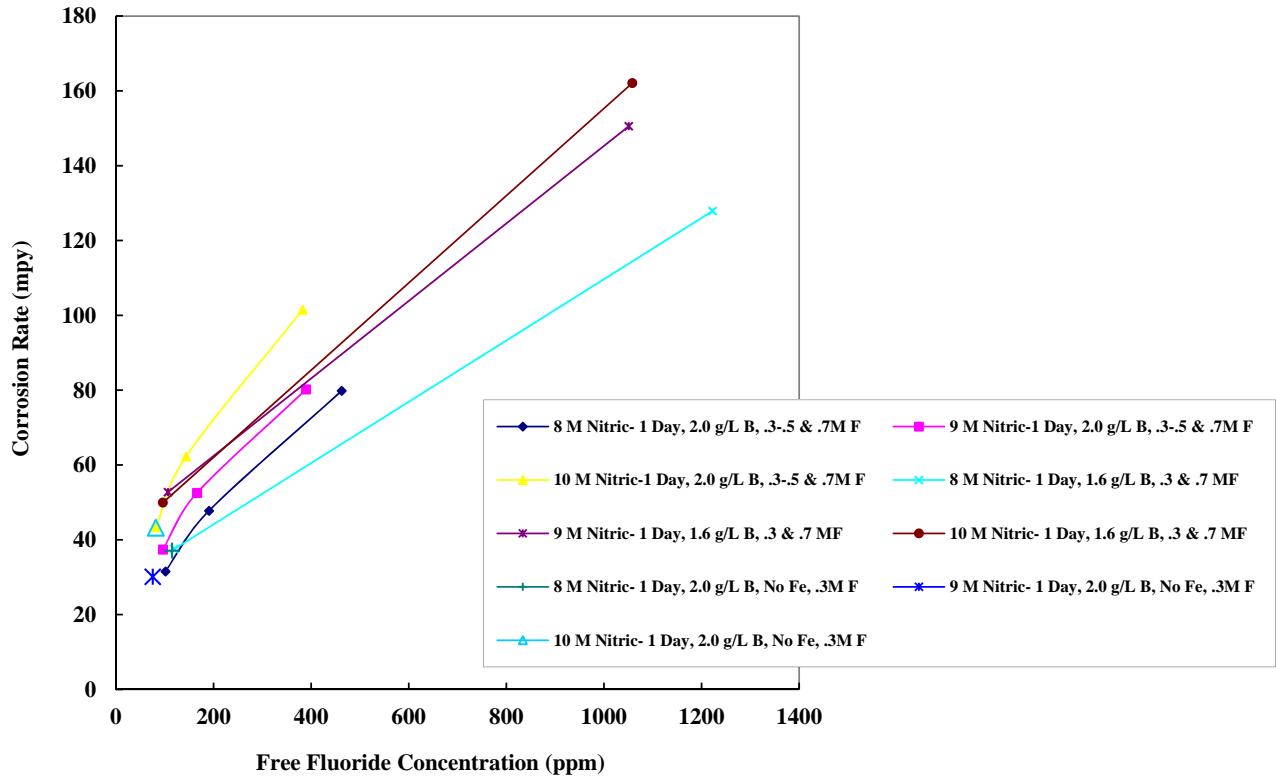


**Figure 6. Corrosion Rate Of 304 Non-welded Coupons Showing The Effect Of Boron and Iron Concentration.**

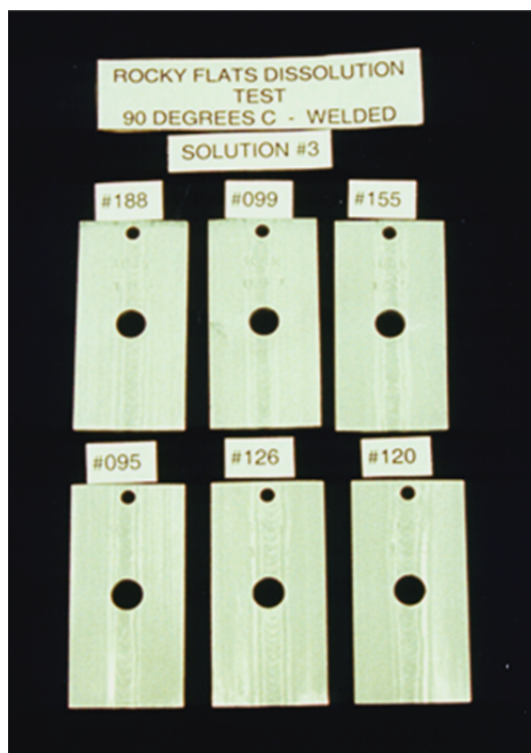


**Figure 7. Representative Welded Coupons (Tested In 10M HNO<sub>3</sub>, 0.18M Fe, 2.0 g/l B, 0.2-0.7M F<sup>-</sup> @ 90°C)**

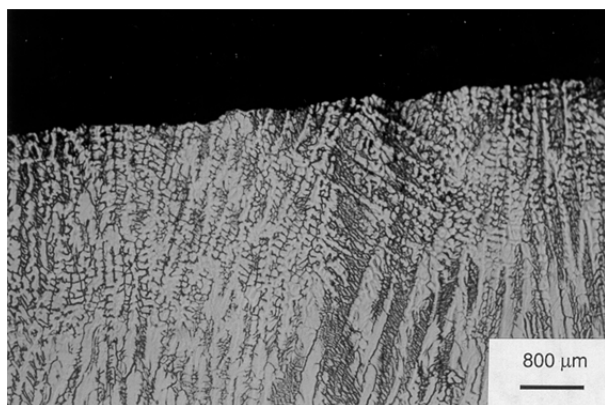


Welded  
Coupon # 84

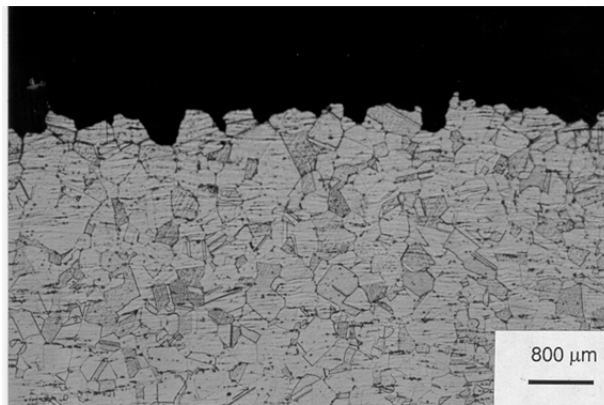


Non-welded  
Coupon # 19

**Figure 8. Welded And Non-welded 304 Coupon (tested 8M HNO<sub>3</sub>, 0.7M F<sup>-</sup>, 1.6 g/l B, 0.18M Fe @ 90°C)**



Weld



Parent Metal

**Figure 9. Transverse Cross Section Of Weld And Parent Metal From Welded 304 Coupon # 84**

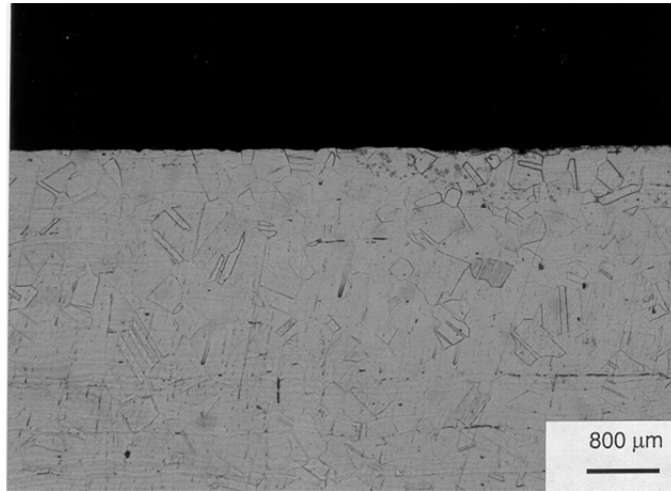


**Figure 10. Transverse Cross Section Of Non-welded 304 Coupon # 19**